Diabetic Complications Consortium

Application Title: Understanding how exposure to maternal diabetes impacts kidney development.

Principal Investigator: Jacqueline Ho

1. Project Accomplishments:

Maternal diabetes has been linked to a 50% increased risk of chronic kidney disease compared to the general population, even with treatment of hyperglycemia. In this study, we have exploited the *Ins2+/C96Y* (also known as Akita) mouse, as a biologically relevant model of maternal diabetes exposure *in utero* which results in a reduction in nephron number in wildtype pups compared to non-maternal diabetes exposed pups. This model more closely resembles the human condition, because it does not result in intrauterine growth restriction, unlike the use of streptozotocin to induce maternal diabetes. In the first aim, we have generated scRNA-seq data from the kidneys of control and maternal diabetes-exposed (DM_Exp) at postnatal day 2 (P2) to describe differential gene expression in these kidneys, as a means of understanding the underlying molecular mechanisms that drive the risk for kidney disease in these animals. In the second aim, we have performed initial renal ischemia-reperfusion injury (IRI) experiments, as a model of acute kidney injury (AKI), in control and DM_Exp. At this point, we are working towards increasing the numbers of animals for these experiments.

2. Specific Aims:

Aim 1: To define the molecular mechanisms underlying the reduction in nephron number associated with exposure to maternal diabetes using state of the art single cell RNA sequencing approaches.

Results: Single cell preparations were made from one control and one DM_Exp kidney at P2, and sent for scRNA-seq targeting 6,000 cells at 25,000 reads/cell (10X Genomics Chromium Controller and Illumina sequencing) to GENEWIZ Inc. Cells exhibited high viability prior to chip loading (>88%). Data processing, quality control and multiplet detection and filtering resulted in 4,867 and 7,686 high-quality cells for the control and DM_Exp kidney respectively. Cells from the control and DM_Exp kidney did not exhibit pronounced differences that would indicate unaccounted-for confounding batch effects (**Figure 1A**) [67], and major structural components of the kidney were clearly visible in low-dimensional representations (4,185 nephron progenitor, 890 distal tubule, 831 proximal tubule and 588 podocyte cells), (**Figure 1B**), with corresponding marker gene expression (data not shown). Focusing on the nephron progenitor lineage (**Figure 2A**), pseudotime analysis using slingshot [68] allowed us to assess gene expression differences across pseudotime for the podocyte, proximal and distal tubular lineages (**Figure 2A**). A generalized additive modeling approach revealed differences of Six2 expression between the DM_Exp and control kidney in the tubular lineages, especially early in differentiation (**Figure 2B**). Together, these data demonstrate that we are able to produce high-quality scRNA-seq data of control and DM_Exp kidneys, and corroborate mild but noticeable Six2 expression differences

between control and DM_Exp, as we have previously published [18]. We are in the process of depositing these data into NCBI GEO.

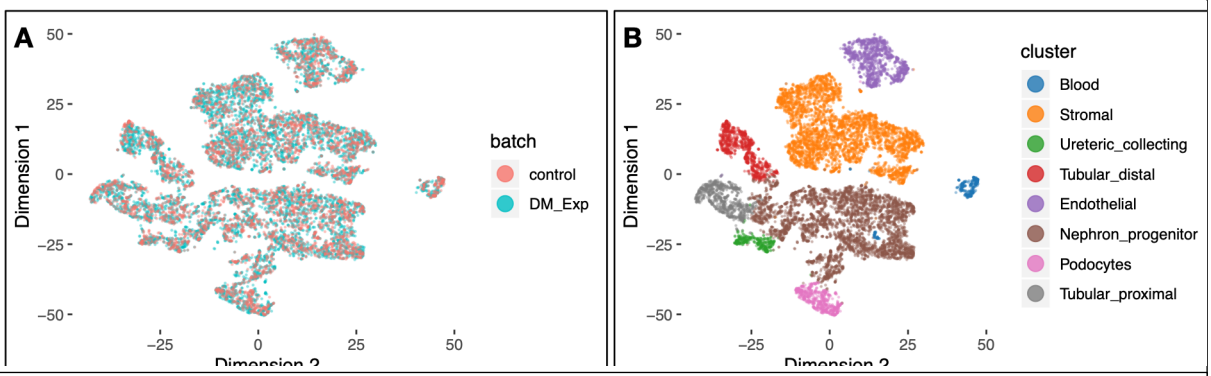

Figure 1: DM_Exp and control kidney scRNAseq reveals similar kidney compartments. Both panels show tSNE embedding of 12,545 cells from two whole kidneys. **(A)** Cells from control (red) and DM_Exp (blue) kidney. **(B)** Clustering of cells from both kidneys demonstrate major structural components of the kidney.

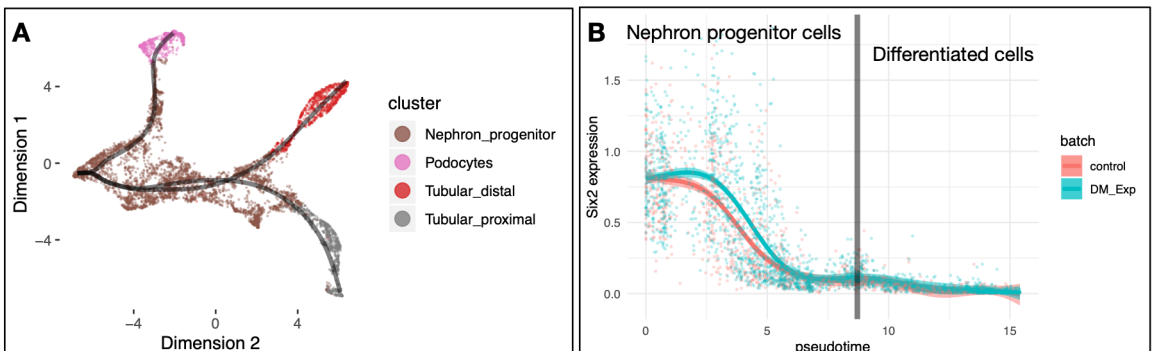

Figure 2: DM_Exp (blue) have increased Six2 expression in nephron progenitors compared to controls (red) via pseudotime. (A) UMAP embedding of nephron cell types (same clusters as in **Figure 1;** together with inferred lineage trajectories). (B) Smoothed [1] Six2 expression across the nephron progenitor to distal tubule lineage. Curves denote smoothed based expression estimates based on a generalized additive model, with confidence bands indicating 2 times the standard error.

Following alignment and clustering analyses, differential expression between control and DM_Exp kidneys at P2 was calculated for each annotated cluster using DESeq2 (version 1.26.0)[1], with its behavior modified for single-cell comparisons as suggested by DESeq2's documentation (http://bioconductor.org/packages/devel/bioc/vignettes/DESeq2/inst/doc/DESeq2.html). Specifically, comparisons were made using the likelihood ratio test (test="LRT"), library size estimates were calculated using the Scran[2] (version 1.14.6) package's calculateSumFactors function, outlier samples were not eliminated (minReplicatesForReplace=Inf), and the lower bound for fitting gene-wise dispersion estimates was set as $1e^{-6}$ (minmu=1e-6). Changes in gene expression were considered significant based on an adjusted p-value cutoff of 0.05. A subset of differentially expressed genes in different cellular compartments (either increased or decreased) in

DM_Exp kidneys compared to control kidneys is displayed in Table 1. We are currently in the midst of validating these data.

Table 1: Differentially expressed genes in DM_Exp compared to control kidneys at P2

	Endothelium	Stromal	Nephron Progenitor	Podocytes	Proximal tubule	Distal tubule
Increased	*Jarid2, BMPR2, Sox11, mt-Nd3*	*mt-Nd3, Dlk1, Fosl2, Fgf9, Pax8, Ly6a, Krt7, Krt8, Epcam, Cldn3, Cldn8, Lrp2, Lcn2*	*Cldn4, Col1a1, Col3a1, Muc1, mt-Nd3, Aqp2*	*mt-Nd3, Efnb2*	*mt-Nd3, Slc16a5, Tmem65*	*Aqp11, mt-Nd3, Slc3a1, Slc5a1, Slc5a8, Slc5a9, Slc6a13, Slc6a18, Slc6a19*, Slc6a20b*, Slc13a2, Slc13a3, Slc16a4, Slc17a1, Slc17a3, Slc18a1, Slc22a1, Slc22a2, Slc22a6, Slc22a12, Slc22a13, Slc22a19, Slc22a27, Slc22a29, Slc22a30, Slc25a10, Slc25a45, Slc26a1, Slc30a1, Slc33a1, Slc51b*
Decreased	*Yam1, Rtp4, Isg15, Ogfr, Ccnb2, Isg15*	*Yam1, Isg15, Bmp4, Slit3*	*Yam1, Dab1, Pdgfrl, Isg15, Dkk1, Hes5, Col5a2, Vcam1*	*Yam1, Fos, Angptl2, Bambi*	*Yam1, Junb, Jun, Fos, Fosb, Hes1, Egr1*	*Yam1, Vcan, Cited2, Osr2, Igfbp2, Klf2, Klf6, Klf7, Jun, Casp6, Dusp6, Bmp4, Ift74, Hes1, Pdgfa, Fos, Aldh1a2, Vcam1, Smad7, Ccnd1, Gas8, Igfbp6, Hoxb3, Dusp1, Krt18, Lhx1, Pdgfc*

Aim 2: To evaluate the functional consequences of the reduction in nephron number in response to a high salt diet and acute kidney injury.

Results:

Renal IRI was performed in 8-12 week old male DM_Exp mice and corresponding controls. In brief, the animals were anesthetized and body temperature maintained at 37^{o}C. The left kidney was clamped using an atraumatic microaneurysm clip for 18-20 min, and reperfusion was visualized. Six days after renal IRI, a nephrectomy was performed of the contralateral right kidney via a midline laparotomy (in our experience, this has improved survival rates compared to simultaneous nephrectomy at the time of IRI). At seven days after renal IRI, the mice were anesthetized with isoflurane for blood collection via cardiac puncture, and the kidneys harvested for subsequent histology, qPCR and Western studies. At this point, we have performed tittering experiments that demonstrate that 18 min of renal IRI results in significant renal injury to both control and DM_Exp animals. Moreover, histologically, there appears to be increased tubular damage in DM_Exp kidneys compared to controls, as evidenced by more tubular dilation and loss of the proximal tubule brush border (Figure 3). This finding will need to be confirmed with additional animals.

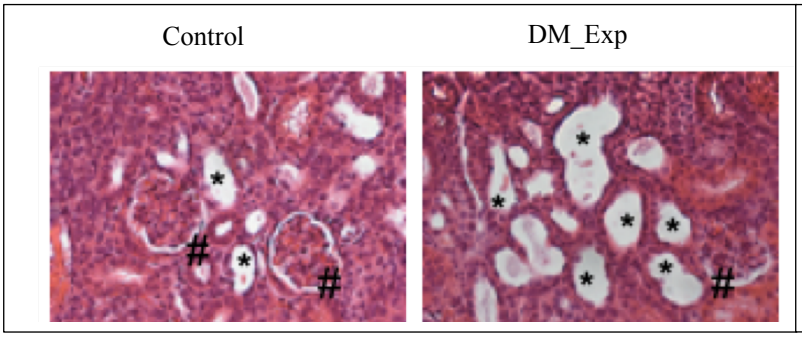

Figure 3. Hematoxylin and eosin (H&E)-stained sections from control and DM_Exp animals showed increased tubular dilation (*) in DM_Exp kidneys. Control and DM_Exp animals underwent 18 min of renal IRI and kidneys collected 7 days after injury. #: glomeruli, scale = 50μm

3. **Publications:** None.